J. Astrophys. Astr. (1995) **16**, 357–374

Disk Luminosity and Angular Momentum for Accreting, Weak Field Neutron Stars in the 'Slow' Rotation Approximation

Bhaskar Datta[1], Arun V. Thampan & Paul J. Wiita[2] *Indian Institute of Astrophysics, Bangalore 560 034, India.*
[1]*Visiting Professor: Raman Research Institute, Bangalore 560 080 India.*
[2]*Permanent address: Department of Physics & Astronomy, Georgia State University, Atlanta, GA 30303–3083, USA.*

Received 1995 June 29; accepted 1995 August 22

Abstract. For accretion on to neutron stars possessing weak surface magnetic fields and substantial rotation rates (corresponding to the secular instability limit), we calculate the disk and surface layer luminosities general relativistically using the Hartle & Thorne formalism, and illustrate these quantities for a set of representative neutron star equations of state. We also discuss the related problem of the angular momentum evolution of such neutron stars and give a quantitative estimate for this accretion driven change in angular momentum. Rotation always increases the disk luminosity and reduces the rate of angular momentum evolution. These effects have relevance for observations of low-mass X-ray binaries.

Key words: Stars: accretion—stars: accretion disks—stars: neutron—stars: rotation.

1. Introduction

Disk accretion on to a neutron star possessing a weak surface magnetic field ($B \lesssim 10^8$ *G*) provides interesting X-ray emission scenarios, and is relevant for understanding X-ray bursters and low-mass X-ray binaries (e.g. van Paradijs 1991). Such weak-field neutron stars can rotate very rapidly and are also seen as millisecond pulsars (Radhakrishnan & Srinivasan 1982; Alpar *et al.* 1982; Bhattacharya & van den Heuvel 1991) and may be relevant for quasi-periodic oscillators (QPOs) (Priedhorsky 1986; Paczyński 1987). The equation of state of neutron star matter as well as general relativity play essential roles in such a scenario. This is in contrast to the strongly magnetic ($B \gtrsim 10^{12}$ *G*) accreting neutron stars, where plasma processes dominate (e.g., Ghosh & Lamb 1991). For the weak-field case, the radius of the innermost stable circular orbit ($r_{\rm orb}$) plays a central role, deciding quantities of observational interest such as the disk luminosity. The relevance of this parameter ($r_{\rm orb}$) was emphasized by Kluźniak & Wagoner (1985, hereafter KW), who pointed out that for weak-field accreting neutron stars it is incorrect to always make the usual assumption that the accretion disk extends very close to the surface of the star, and is separated from it by a thin boundary layer. Using Schwarzschild geometry, Syunyaev & Shakura (1986, hereafter SS) concluded that the boundary layer brushing the neutron star surface will be substantially more X-ray luminous than the extended accretion disk. If the star's radius (R) is less than $r_{\rm orb}$, the

boundary layer is likely to be characterized by poorly collimated tangential motion of the infalling matter and a comparatively soft emission spectrum. Whether or not R exceeds r_{orb} (and consequently the detailed features of the accretion scenario) depends on the geometry of the spacetime and also the equation of state of neutron star matter.

An important aspect of disk accretion on to weak-field neutron star is the possibility that the neutron star will get spun up to very short rotation periods ($\lesssim$ millisecond) over a time of the order of hundreds of millions of years. For such rapid rates of rotation, the relativistic effect of dragging of inertial frames in the vicinity of the neutron star will be important. This effect will alter the trajectories of infalling particles as compared to the non-rotational case. Therefore, for a quantitative description of the accretion features, one must take into account the relativistic effects of rotation upon the spacetime geometry. Although the possible importance of such effects was stressed by KW and SS, the details were not worked out by them.

In this paper we address this question and calculate the disk and surface layer luminosities incorporating the rotational effects in a general relativistic framework. We take the spun up neutron star to be rotating at a particular value, namely, the secular instability limit so as to illustrate the maximal reasonable effects of rotation. This corresponds to the late stages of accretion. We use the Hartle & Thorne (1968; hereafter HT) formalism, for our purpose; this formalism describes a rotationally perturbed Schwarzschild space-time. The HT formalism is valid for strong gravitational fields but only in the limit of uniform rotation with a rate that is 'slow' compared to the critical speed for centrifugal break-up. Neutron star models rotating at the secular instability limit (assuming the star to be homogeneous), relevant in the context of accretion induced spun up neutron stars, are within this limit (Datta & Ray 1983), so this approximation will usually be adequate. Recently Cook *et al.* (1994a & b) calculated last stable orbits of rotating neutron stars incorporating higher order rotational terms that go beyond the HT approximation. However, these authors did not use their results to estimate the disk luminosity and angular momentum evolution involved in the accretion scenario. Although the Hartle & Thorne prescription assumes rotationally perturbed geometry, the use of this prescription provides a first estimate, which is amenable to a straightforward numerical treatment, of the luminosity values and angular momentum evolution for an accreting weak-field neutron star. This can be quite useful in observational applications such as low-mass X-ray binaries. Our calculations are done for a range of stable neutron star configurations computed using a representative sample of the proposed equations of state of neutron star matter. We also consider the accretion driven evolution of the angular momentum of the neutron star in a more accurate fashion than was done by KW.

2. Accretion on to a rotating neutron star

To describe the spacetime around a rotating neutron star we use the metric suggested by Hartle & Thorne (1968). This metric describes a rotationally perturbed Schwarzschild geometry to order Ω^2, where Ω is the angular velocity of the star as seen by a distant observer. The general form of the metric is (signature: $+ - - -$)

$$\begin{aligned} ds^2 &= g_{\alpha\beta}dx^\alpha dx^\beta, (\alpha,\beta = 0,1,2,3) \\ &= e^{2\Phi}dt^2 - e^{2\psi}(d\phi - \omega dt)^2 - e^{2\mu}d\theta^2 - e^{2\lambda}dr^2 + \mathcal{O}(\Omega^3/\Omega_c^3). \end{aligned} \tag{1}$$

Here ω is the angular velocity of the cumulative dragging of inertial frames and $\Omega_c = (GM/R^3)^{1/2}$, the critical angular velocity for equatorial mass shedding, where M and R are the mass and radius of the non-rotating neutron star. For simplicity, we use the geometric units: $c = 1 = G$. The metric components correspond to an interior with the identification:

$$e^{2\Phi} = e^{2\nu}\{1 + 2(h_0 + h_2 P_2)\}, \tag{2}$$

$$e^{2\psi} = r^2 \sin^2\theta\{1 + 2(v_2 - h_2)P_2\}, \tag{3}$$

$$e^{2\mu} = r^2\{1 + 2(v_2 - h_2)P_2\}, \tag{4}$$

$$e^{2\lambda} = \frac{1 + 2(m_0 + m_2 P_2)/(r - 2m)}{1 - 2m/r}, \tag{5}$$

(where 2ν is the gravitational potential function for the non-rotating star and m is the gravitational mass contained within a volume of radius r) and to an exterior with the identification:

$$e^{2\Phi} = e^{-2\lambda} = 1 - 2\frac{M'}{r} + 2\frac{J^2}{r^4}, \tag{6}$$

$$e^{2\psi} = r^2 \sin^2\theta, \tag{7}$$

$$e^{2\mu} = r^2. \tag{8}$$

Here M' and J are respectively the mass and angular momentum of the rotating configuration of the star. The quantity P_2 is the Legendre polynomial of order 2, and h_0, h_2, m_0, m_2, v_2 are all functions of r that are proportional to Ω^2 (see HT). The metric has the desirable property that the internal and external forms match at the surface of the star. For our purpose here, we shall retain only the spherical deformation terms (characterized by subscript 0) and neglect the quadrupole deformation terms (characterized by subscript 2). The latter are necessary for computing stellar quadrupole deformation, but average out in calculating the rotation induced changes to M and R. The applicability of the metric (1) is valid for Ω small in comparison to Ω_c, and to go beyond that approximation requires a treatment similar to that of Cook *et al.* (1994a, b).

A relativistic effect of rotation, important for the astrophysical scenario that we consider here, is the dragging of inertial frames, which implies

$$\bar{\omega}(r) \neq \Omega, \tag{9}$$

where $\bar{\omega}(r)$ is the angular velocity of the stellar fluid relative to the local inertial frame, and is given by (HT)

$$\frac{\mathrm{d}}{\mathrm{d}r}\left(r^4 j \frac{\mathrm{d}\bar{\omega}}{\mathrm{d}r}\right) + 4r^3\bar{\omega}\frac{\mathrm{d}j}{\mathrm{d}r} = 0, \tag{10}$$

where

$$j(r) = e^{-\nu}(1 - 2m/r)^{1/2}, \tag{11}$$

with the boundary conditions

$$\left(\frac{\mathrm{d}\bar{\omega}}{\mathrm{d}r}\right)_{r=0} = 0; \quad \bar{\omega}(r = \infty) = \Omega. \tag{12}$$

For $r > R$(i.e., outside the star),

$$\bar{\omega}(r) = \Omega - 2J/r^3, \tag{13}$$

where J is the angular momentum of the star:

$$J = \frac{R^4}{6}\left(\frac{\mathrm{d}\bar{\omega}}{\mathrm{d}r}\right)_{r=R}. \tag{14}$$

The equations of motion are derived from the Lagrangian corresponding to the metric (1):

$$\mathscr{L} = \tfrac{1}{2}\{e^{2\Phi}\dot{t}^2 - e^{2\lambda}\dot{r}^2 - e^{2\mu}\dot{\theta}^2 - e^{2\psi}(\dot{\phi} - \omega\dot{t})^2\}, \tag{15}$$

where a dot represents a derivative with respect to proper time. We shall, for purpose of illustration, take the polar angle (θ) to be fixed and equal to $\pi/2$, which corresponds to the equatorial plane.

The metric (1) and the equations of motion provide three equations in the three variables $\dot{\phi}$, $\dot{t}$, and $\dot{r}$. From these, we can get (see KW)

$$\dot{r}^2 = \tilde{E}^2 - 2\omega\tilde{E}\tilde{l} - h^2(1 + \tilde{l}^2/r^2), \tag{16}$$

where

$$\tilde{E} = h^2\dot{t} + \omega r^2\dot{\phi}, \tag{17}$$

and

$$\tilde{l} = r^2(\dot{\phi} - \omega\dot{t}), \tag{18}$$

stand respectively for the energy and angular momentum per unit rest mass (denoted by m_B) and

$$h = (1 - 2M'/r)^{1/2}. \tag{19}$$

The conditions for the turning point of the motion, the extremum of the energy, and the minimum of the energy are respectively given by (see Misner, Thorne & Wheeler 1974)

$$\tilde{E}^2 = V^2, \tag{20}$$

$$\frac{\mathrm{d}\tilde{E}}{\mathrm{d}r} = 0 = \frac{\mathrm{d}V}{\mathrm{d}r}, \tag{21}$$

and

$$\frac{\mathrm{d}^2\tilde{E}}{\mathrm{d}r^2} > 0, \tag{22}$$

where V is the effective potential, given by

$$V^2 = 2\omega\tilde{E}\tilde{l} + h^2(1 + \tilde{l}^2/r^2). \tag{23}$$

For marginally stable orbits we can use the condition

$$\frac{\mathrm{d}^2\tilde{E}}{\mathrm{d}r^2} = 0 = \frac{\mathrm{d}^2V}{\mathrm{d}r^2}. \tag{24}$$

Written explicitly, equations (20), (21), and (24) respectively become

$$\tilde{E}^2 - \frac{\tilde{j}a\tilde{E}}{x^3} - \left(1 - \frac{1}{x}\right)\left(1 + \frac{a^2}{x^2}\right) = 0, \tag{25}$$

$$a^2 + \frac{3\tilde{j}a\tilde{E}}{(2x-3)} - \frac{x^2}{(2x-3)} = 0, \tag{26}$$

$$x^2 - 3a^2x + 6(a^2 - \tilde{j}a\tilde{E}) = 0, \tag{27}$$

where $x = r/2M'$, the dimensionless radial co-ordinate; $\tilde{j} = J/M'^2$ and $a = \tilde{l}/2M'$ are the dimensionless angular momenta for the star and the infalling matter respectively. Solving equations (25)–(27) simultaneously gives the values for the energy ($E_{\rm orb}$) and the specific angular momentum ($a_{\rm orb}$) of the accreted particle in the innermost stable orbit having a radius $x = x_{\rm orb}$.

Using Schwarzschild geometry, it was shown by SS that an accretion disk whose luminosity is small compared to the Eddington limit can exist only for R greater than the radius of the last stable circular orbit, $3r_g$, where $r_g = 2M$ = the Schwarzschild radius. For $R < 3r_g$, the accreting matter falling on to the neutron star will follow the trajectory of a free particle in this geometry, with an energy equal to $m_B\sqrt{8/9}$. These authors also gave estimates of the energy released in the disk and in the boundary layer for R/r_g ranging from 1·5 to 10 without reference to any specific equation of state model. In the case where the neutron star has a high spin rate, the innermost stable orbit was calculated by KW using the HT metric to describe rotating spacetime. These authors, however, did not estimate the luminosity, and they neglected the rotational corrections to M and R in computing the evolution of angular momentum.

For a low-field, accreting neutron star possessing substantial rotation, the luminosity from the disk accretion can be calculated using equations (25)–(27). We use here the notation $x^* = R'/2M'$, where M' and R' correspond to the neutron star mass and radius that include corrections due to the rotation. The following distinct cases are possible:

2.1 *Case (a): Radius of the star is greater than* $r'_{\rm orb}$

If an accretion disk were to form around a relatively large neutron star (i.e., $x^* > x_{\rm orb}$), the ingress of a particle of rest mass m_B from infinity to the inner disk boundary will release an amount of energy given by

$$E'_D = m_B\{1 - \tilde{E}_k(x^*)\}, \tag{28}$$

where $\tilde{E}_k(x^*)$ stands for the specific energy of the particle in the stable orbit just above the surface, obtained by solving equations (25) and (26) numerically for $x = x^*$. The energy loss in the boundary layer will be

$$E'_S = m_B\{\tilde{E}_k(x^*) - \tilde{E}_0(x^*)\}, \tag{29}$$

where $\tilde{E}_0(x^*)$ is the energy of the particle at rest on the surface of the neutron star, which can be calculated from equation (25) for $x = x^*$ and the specific angular momentum at the star's surface.

2.2 *Case (b): Radius of the star is smaller than* $r'_{\rm orb}$

In this case, $x^* < x_{\rm orb}$ and the accretion disk will extend inward to a radius corresponding to $x = x_{\rm orb}$. Now the energy released in the disk as the particle comes in from infinity to the innermost stable orbit will be

$$E'_D = m_B\{1 - \tilde{E}_{\rm orb}\}, \tag{30}$$

and the energy released in the boundary layer will be

$$E'_S = m_B\{\tilde{E}_{\rm orb} - \tilde{E}_0(x^*)\}. \tag{31}$$

A remark about the boundary layer luminosity formula that we use, is in order here. Although this formula gives a plausible estimate for the boundary layer luminosity, strictly speaking, it is an overestimate as it does not take into account the subtraction of the energy that goes into spinning up of the neutron star. The need for such a correction was pointed out by Kluźniak (1987) and quantitative estimates for this were suggested by Ghosh, Lamb & Pethick (1977), Papaloizou & Stanley (1986), and Kley (1991). A fairly simple and general way to estimate the same was given recently by Popham & Narayan (1995) who considered the accretion disk boundary layer problem in cataclysmic variables. Significantly, these authors have stressed that most of the decrease in the boundary layer luminosity will occur in the early stages of spin-up, when the star is rotating slowly, *rather* than the late stages when it is approaching limiting break up rotation rates. The scenario that we consider in this paper corresponds to the latter stage. Therefore, for our purpose, the formula for the boundary layer luminosity that we have used is expected to be adequate. This point is elaborated in § 4.

3. Equation of state and rotation-induced changes in structure

The structure of neutron stars depends sensitively on the equation of state at high densities, especially for density regions $\gtrsim 10^{14}\,{\rm g\,cm^{-3}}$. There is no general consensus on the exact behaviour of the equation of state at these high densities. For our purpose here we choose the following six equations of state: (1) Pandharipande (N) (neutron matter) model, based on the lowest order constrained variational method using Reid potentials (Pandharipande 1971a); (2) Pandharipande (Y) (1971b) hyperonic matter; (3) Bethe-Johnson model V (N) for neutron matter (Bethe & Johnson 1974) which uses improved phenomenological potentials; (4) Walecka (1974) model for neutron matter, using scalar-vector interactions in a field theoretical framework; (5) Wiringa UV14 + UVII model for neutron-rich matter in beta equilibrium – a variational calculation incorporating the three-body interactions (Wiringa, Fiks & Fabrocini 1988); and (6) neutron-rich matter in beta equilibrium, based on the chiral sigma model (Sahu, Basu & Datta 1993). Of these, models (1) and (2) are 'soft' equations of state and (4) and (6) are rather 'stiff' ones, while the models (3) and (5) are roughly intermediate in 'stiffness'.

The composite equation of state to determine the neutron star structure was constructed by joining the selected high density equation of state to that of Negele & Vautherin (1973) for the density range $(10^{14} - 5 \times 10^{10})\,{\rm g\,cm^{-3}}$, Baym, Pethick & Sutherland (1971) for densities down to $\sim 10^3\,{\rm g\,cm^{-3}}$ and Feynman, Metropolis & Teller (1949) for densities less than $10^3\,{\rm g\,cm^{-3}}$.

For a fixed central density (and a chosen equation of state model), the fractional changes in the gravitational mass ($\Delta M/M$) and radius ($\Delta R/R$) of the neutron star due to the rotation induced spherical deformation are proportional to Ω^2 (Ω is the angular velocity of the star as seen by a distant observer), and can be (numerically) obtained from a knowledge of the radial distributions of the mass and pressure perturbation terms, $m_0(r)$ and $p_0(r)$ (HT; Datta & Ray 1983; Datta 1988). The non-rotating mass (M) and radius (R) are obtained by numerically integrating the relativistic equations for hydrostatic equilibrium (see e.g. Arnett & Bowers 1977). The changes ΔM and ΔR are given by

$$\Delta M = m_0(R) + J^2/R^3, \tag{32}$$

$$\Delta R = -\left.\frac{p_0(\rho + p)}{\mathrm{d}p/\mathrm{d}r}\right|_{r=R}, \tag{33}$$

where $p(r)$ and $\rho(r)$ are the pressure and the total mass-energy density at the radial distance r from the center of the star.

For purpose of estimating the angular momentum evolution of the accreting neutron star (discussed in the next section), we need to know the baryonic mass of the rotating neutron star. The rotation induced change in the baryonic mass (denoted by ΔM_B) is conveniently written as

$$\Delta M_B = \Delta E_B + \Delta M, \tag{34}$$

where ΔE_B is the rotation induced change in the binding energy of the star (HT):

$$\Delta E_B = -J^2/R^3 + \int_0^R 4\pi r^2 B(r)\mathrm{d}r, \tag{35}$$

where

$$\begin{aligned} B(r) = (\rho + p)p_0 &\left\{\frac{\mathrm{d}\rho}{\mathrm{d}p}\left[\left(1 - \frac{2m}{r}\right)^{-1/2} - 1\right] - \frac{\mathrm{d}\varepsilon}{\mathrm{d}p}\left(1 - \frac{2m}{r}\right)^{-1/2}\right\} \\ &+ (\rho - \varepsilon)\left(1 - \frac{2m}{r}\right)^{-3/2}\left[\frac{m_0}{r} + \frac{1}{3}j^2 r^2 \bar{\omega}^2\right] \\ &- \frac{1}{4\pi r^2}\left[\frac{1}{12}j^2 r^4\left(\frac{\mathrm{d}\bar{\omega}}{\mathrm{d}r}\right)^2 - \frac{1}{3}\frac{\mathrm{d}j^2}{\mathrm{d}r} r^3 \bar{\omega}^2\right], \end{aligned} \tag{36}$$

and $\varepsilon = \rho - m_B n$ is the density of internal energy, with $n(r)$ and m_B denoting respectively, the baryonic density and rest mass.

Density profiles of neutron stars are remarkably flat out to $r = (0{\cdot}8\text{–}0{\cdot}85)R$ (Datta *et al.* 1995). Therefore, the concept of rotational secular instability in the context of Maclaurin spheroids (Chandrasekhar 1969) is a relevant approximation when considering the rotational stability of neutron stars. For a uniformly rotating homogeneous spheroid, this instability corresponds to an angular velocity $\Omega = \Omega_s$, given by

$$\frac{\Omega_s^2}{2\pi G\bar{\rho}} = 0{\cdot}18, \tag{37}$$

where $\bar{\rho}$ is the average density of the star. The quantity Ω_s sets a rough limit up to which the neutron star can be spun up, before the onset of rotational instabilities.

Table 1. Changes in Neutron Star Properties due to Rotation.

EOS Model (1)	ρ_c (g cm^{-3}) (2)	$M/M_\odot$ (3)	R (km) (4)	Ω_s ($rad\ s^{-1}$) (5)	$\Delta M/M$ (6)	$\Delta R/R$ (7)	r_{orb} (km) (8)	r'_{orb} (km) (9)
Pandharipande (N)	$1.24E15$	1.062	10.390	$5.82E3$	0.085	0.033	9.408	7.936
	$1.50E15$	1.241	10.150	$6.52E3$	0.080	0.029	10.990	9.244
	$1.75E15$	1.367	9.936	$7.07E3$	0.076	0.025	12.110	10.140
	$1.83E15$	1.400	9.867	$7.23E3$	0.074	0.024	12.400	10.360
	$3.88E15$	1.658	8.585	$9.69E3$	0.054	0.011	14.690	11.860
Pandharipande (Y)	$2.18E15$	1.045	8.767	$7.45E3$	0.073	0.029	9.257	7.817
	$3.26E15$	1.289	8.096	$9.33E3$	0.064	0.019	11.420	9.477
	$3.88E15$	1.354	7.796	$1.01E4$	0.059	0.016	11.990	9.855
	$4.79E15$	1.400	7.437	$1.10E4$	0.054	0.012	12.400	10.070
	$5.74E15$	1.414	7.153	$1.18E4$	0.050	0.010	12.530	10.080
Bethe–Johnson V (N)	$9.50E14$	1.003	11.100	$5.12E3$	0.089	0.035	8.885	7.470
	$1.24E15$	1.292	10.830	$6.04E3$	0.084	0.029	11.450	9.627
	$1.25E15$	1.303	10.820	$6.08E3$	0.084	0.029	11.540	9.712
	$1.37E15$	1.400	10.690	$6.41E3$	0.081	0.027	12.400	10.410
	$2.18E15$	1.683	10.020	$7.75E3$	0.067	0.018	14.910	12.280
	$3.26E15$	1.757	9.304	$8.84E3$	0.057	0.012	15.560	12.620

Table 1. (continued).

EOS Model (1)	ρ_c (g cm^{-3}) (2)	$M/M_\odot$ (3)	R (km) (4)	Ω_s ($rad\ s^{-1}$) (5)	$\Delta M/M$ (6)	$\Delta R/R$ (7)	r_{orb} (km) (8)	r'_{orb} (km) (9)
Walecka	$6.50E14$	1.035	12.200	$4.52E3$	0.098	0.037	9.168	7.682
	$7.48E14$	1.279	12.240	$5.00E3$	0.095	0.033	11.330	9.522
	$7.75E14$	1.342	12.240	$5.12E3$	0.094	0.032	11.890	9.994
	$8.02E14$	1.400	12.240	$5.23E3$	0.094	0.031	12.400	10.430
	$2.18E15$	2.243	11.060	$7.71E3$	0.059	0.009	19.870	15.850
Wiringa UV14 + UVII	$8.50E14$	1.053	11.110	$5.25E3$	0.095	0.035	9.328	7.837
	$9.72E14$	1.282	11.120	$5.78E3$	0.092	0.031	11.360	9.550
	$1.00E15$	1.330	11.120	$5.88E3$	0.091	0.031	11.780	9.899
	$1.04E15$	1.400	11.120	$6.04E3$	0.090	0.028	12.400	10.410
	$2.70E15$	2.188	9.875	$9.02E3$	0.053	0.004	19.380	15.120
Chiral Sigma Model	$3.50E14$	1.017	14.320	$3.52E3$	0.109	0.041	9.009	7.463
	$3.85E14$	1.261	14.620	$3.80E3$	0.110	0.038	11.170	9.345
	$4.00E14$	1.360	14.740	$3.90E3$	0.110	0.037	12.050	10.110
	$4.06E14$	1.400	14.780	$3.94E3$	0.109	0.037	12.400	10.400
	$1.26E15$	2.592	14.220	$5.68E3$	0.069	0.015	22.960	18.670

Table 2. Disk and Boundary Layer Luminosities.

EOS Model (1)	$M/M_\odot$ (2)	$M'/M_\odot$ (3)	E_D (m_0c^2) (4)	E'_D (m_0c^2) (5)	$\Delta E/E$ (6)	E_S (m_0c^2) (7)	E'_S (m_0c^2) (8)	$\Delta E/E$ (9)
Pandharipande (N)	1.062	1.152	0.056	0.066	0.1687	0.108	0.105	−0.0259
	1.298	1.400	0.057	0.073	0.2841	0.156	0.148	−0.0523
	1.400	1.504	0.057	0.074	0.2969	0.181	0.172	−0.0473
	1.642	1.738	0.057	0.075	0.3126	0.269	0.259	−0.0378
	1.658	1.748	0.057	0.075	0.3174	0.287	0.276	−0.0391
Pandharipande (Y)	1.045	1.121	0.057	0.071	0.2379	0.138	0.130	−0.0534
	1.289	1.371	0.057	0.074	0.2926	0.215	0.206	−0.0431
	1.319	1.400	0.057	0.074	0.2957	0.228	0.218	−0.0423
	1.400	1.476	0.057	0.075	0.3099	0.276	0.266	−0.0395
	1.414	1.485	0.057	0.075	0.3176	0.298	0.285	−0.0409
Bethe–Johnson V (N)	1.003	1.092	0.053	0.060	0.1347	0.090	0.089	−0.0112
	1.292	1.400	0.057	0.072	0.2542	0.138	0.132	−0.0461
	1.400	1.513	0.057	0.074	0.2919	0.160	0.152	−0.0511
	1.576	1.691	0.057	0.075	0.3030	0.200	0.191	−0.0427
	1.757	1.857	0.057	0.075	0.3155	0.278	0.267	−0.0381

Table 2. (continued).

EOS Model (1)	$M/M_\odot$ (2)	$M'/M_\odot$ (3)	E_D (m_0c^2) (4)	E'_D (m_0c^2) (5)	$\Delta E/E$ (6)	E_S (m_0c^2) (7)	E'_S (m_0c^2) (8)	$\Delta E/E$ (9)
Walecka	1.035	1.136	0.051	0.058	0.1298	0.083	0.083	0.0001
	1.279	1.400	0.057	0.067	0.1905	0.112	0.109	−0.0218
	1.400	1.531	0.057	0.071	0.2399	0.129	0.124	−0.0352
	1.680	1.825	0.057	0.075	0.3123	0.173	0.165	−0.0441
	2.243	2.375	0.057	0.077	0.3405	0.309	0.299	−0.0342
Wiringa UV14 + UVII	1.053	1.153	0.055	0.063	0.1541	0.097	0.096	−0.0114
	1.282	1.400	0.057	0.071	0.2430	0.131	0.126	−0.0384
	1.400	1.526	0.057	0.074	0.2896	0.150	0.144	−0.0439
	1.680	1.817	0.057	0.075	0.3148	0.201	0.194	−0.0359
	2.188	2.305	0.057	0.078	0.3653	0.355	0.342	−0.0369
Chiral Sigma Model	1.017	1.128	0.045	0.051	0.1140	0.066	0.067	0.0189
	1.261	1.400	0.052	0.059	0.1455	0.085	0.085	0.0075
	1.400	1.553	0.055	0.064	0.1686	0.097	0.097	−0.0010
	1.644	1.817	0.057	0.070	0.2260	0.120	0.118	−0.0224
	2.592	2.771	0.057	0.076	0.3274	0.263	0.255	−0.0324

The prescription mentioned earlier to calculate the mass and radius of a rotating relativistic star is valid only for rotation rates that are 'slow' in comparison to Ω_c. Hartle & Thorne (1968) constructed 'slowly' rotating neutron star models all the way up to $\Omega = \Omega_c$ for the Harrison-Wheeler and Tsuruta-Cameron equations of state. Here we shall only consider rotating neutron stars with $\Omega = \Omega_s$ because of the secular instability consideration, and will employ the newer equation of state models mentioned earlier; these models will then illustrate the maximal reasonable effects of rotation. Since $\Omega_s = (0{\cdot}27)^{1/2}\,\Omega_c$, the models constructed by us are adequately treated in the limit of 'slow' rotation. To treat the maximal *possible* effects of rotation, one has to go beyond this limit, and use a technique similar to that employed by Cook *et al.* (1994a, b) for very rapidly (but still uniformly) rotating neutron stars; they determined that spin-up to the millisecond pulsar regime is possible for a wide range of equations of state.

4. Results and conclusions

In Table 1 we give the neutron star properties calculated for the various equations of state as a function of the central density (ρ_c). Columns (3) and (4) list the non-rotating mass and radius. Column (5) gives the corresponding value of Ω_s and columns (6) and (7) give the differences between the rotating and non-rotating neutron star mass and radius. Column (8) gives the non-rotating values of $r_{\rm orb}$ while column (9) shows how $r_{\rm orb}$ decreases due to rotation. Typical increases in mass are (5–11)%, in radius $\leqslant 4\%$, while $r_{\rm orb}$ decreases between 15% and 25%.

In the second and third columns of Table 2 we give values of the non-rotating mass M and the rotationally enhanced mass M' for a maximal reasonable rotation rate ($\Omega = \Omega_s$). Columns (4) and (7) show the disk and boundary layer luminosities for non-rotating configurations (E_D and E_S respectively). The values of E'_D and E'_S, including rotational effects treated consistently within the HT framework, are given in columns (5) and (8). All values of luminosity listed in the table are in units of the baryonic rest mass. The boundary layer luminosity values listed in Table 2 do not include corrections for the energy that goes into spinning up the neutron star. We have made estimate of this correction following the prescription of Popham & Narayan (1995) for the case of $1{\cdot}4\,M_\odot$ neutron star corresponding to the EOS model by Wiringa *et al.* (1988). This is shown in Fig. 1 which is a plot of the rotational energy correction $E_{\rm rot}$ in units of the particle rest mass vs. the stellar rotation rate Ω. It is clear from this figure that the rotational energy correction to the boundary layer luminosity tends to become unimportant as the angular velocity approaches very high values. For $\Omega = \Omega_s$, $E_{\rm rot} \sim 0{\cdot}048$; this is an order of magnitude less than the boundary layer luminosity given in Table 2. Therefore the neglect of rotational energy correction to calculate E'_s for the neutron star rotating at the limiting Ω as considered by us does not result in a gross overestimate.

We find that as M' increases, the luminosity in the boundary layer increases monotonically. The disk luminosity increases in the rotational case as compared to the static case; the increase, illustrated in column (6), is most significant ($\gtrsim 30\%$) for high M' values. The fractional changes $\Delta E_s/E_s$ values (column (9)), however, exhibit a non-monotonic behaviour with increasing M', though they typically decrease by a few per cent. Further, as is well known, we see that the radius of the innermost stable orbit is less than the static case (where $r_{\rm orb} = 6M$) for all equations of state considered.

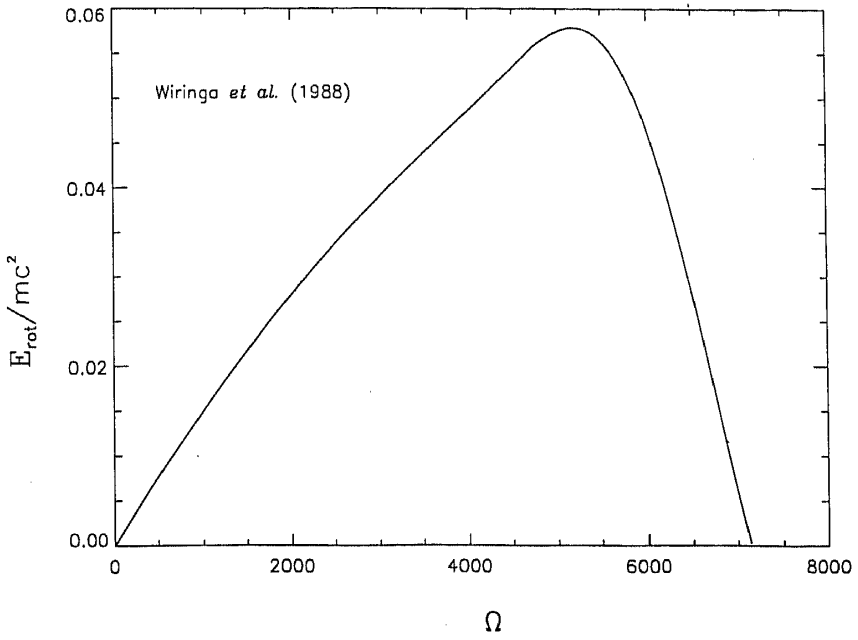

Figure 1. Rotational energy correction $E_{\rm rot}/mc^2$ to the boundary layer luminosity as a function of the stellar rotation rate Ω.

We now make a few remarks about the angular momentum evolution of the accreting neutron star. In performing the angular momentum evolution calculations, we have made the following additional assumptions:

- The central density of the neutron star does not change with mass accretion. This is a reasonable assumption to make because for a static, stable neutron star, while the central density increases with increasing mass, the rotation tends to 'decrease' the central density. Thus if the total accreted mass is not large, the effect of rotation will nearly compensate for the effect of accretion on the central density;
- The mass accretion rate is equal to dM_B/dt as in KW, but with the difference that rotational effects have been taken into account, that is, $M_{\rm acc} = dM'_B/dt$;
- The maximum angular momentum for a particular neutron star configuration is determined by the secular instability limit:

$$\Omega = \Omega_s = (0{\cdot}27)^{1/2}\Omega_c.$$

KW derived the evolution equation

$$\frac{dJ}{dM'} = \tilde{l}(r(M'))\frac{dM'_B}{dM'} = 2M'a\frac{dM'_B}{dM}, \tag{38}$$

and solved it under the simplifying assumptions

$$M' \simeq M; \quad \frac{dM'_B}{dM'} \simeq \frac{dM_B}{dM}.$$

For dM_B/dM, KW used a fit to the values of M and R taken from Arnett & Bowers (1977). Here, we solve equation (38) numerically, incorporating the effect of rotation as

Table 3. Gravitational and Baryonic Masses as Functions of Angular Momentum.

EOS Model (1)	ρ_c (g cm^{-3}) (2)	$M/M_\odot$ (3)	$M'/M_\odot$ (4)	$M'_B/M_\odot$ (5)	J (g cm^2 s^{-1}) (6)
Pandharipande (N)	1.83E15	1.400	1.400	1.567	0.000E00
			1.413	1.578	2.526E48
			1.426	1.589	3.648E48
			1.438	1.599	4.420E48
			1.467	1.623	5.823E48
Pandharipande (Y)	4.79E15	1.400	1.400	1.615	0.000E00
			1.416	1.627	3.269E48
			1.432	1.639	4.660E48
			1.448	1.652	5.772E48
			1.466	1.665	6.746E48
Bethe–Johnson V (N)	1.37E15	1.400	1.400	1.556	0.000E00
			1.420	1.572	3.139E48
			1.440	1.589	4.424E48
			1.460	1.606	5.422E48
			1.500	1.639	6.992E48
Walecka	8.02E14	1.400	1.400	1.671	0.000E00
			1.430	1.699	3.760E48
			1.486	1.750	6.318E48
			1.500	1.764	6.844E48
			1.516	1.779	7.370E48
Wiringa UV14 + UVII	1.04E15	1.400	1.400	1.562	0.000E00
			1.420	1.578	3.050E48
			1.443	1.598	4.538E48
			1.467	1.618	5.655E48
			1.512	1.656	7.291E48
Chiral Sigma Model	4.06E14	1.400	1.400	1.521	0.000E00
			1.434	1.549	3.975E48
			1.472	1.581	5.760E48
			1.505	1.609	6.976E48
			1.539	1.638	8.031E48

outlined above. We assume that for a central density that gives a gravitational mass of $1{\cdot}4\,M_\odot$ in the non-rotating case, $J = \Omega = 0$, and we then vary Ω from zero to Ω_s. The results are presented in Table 3; these should be compared with Table 1 of KW.

From Table 3, we see that for each equation of state, a plot of M'_B vs M' gives an almost constant slope. We solve equation (38) using the boundary condition $J = 0$ for

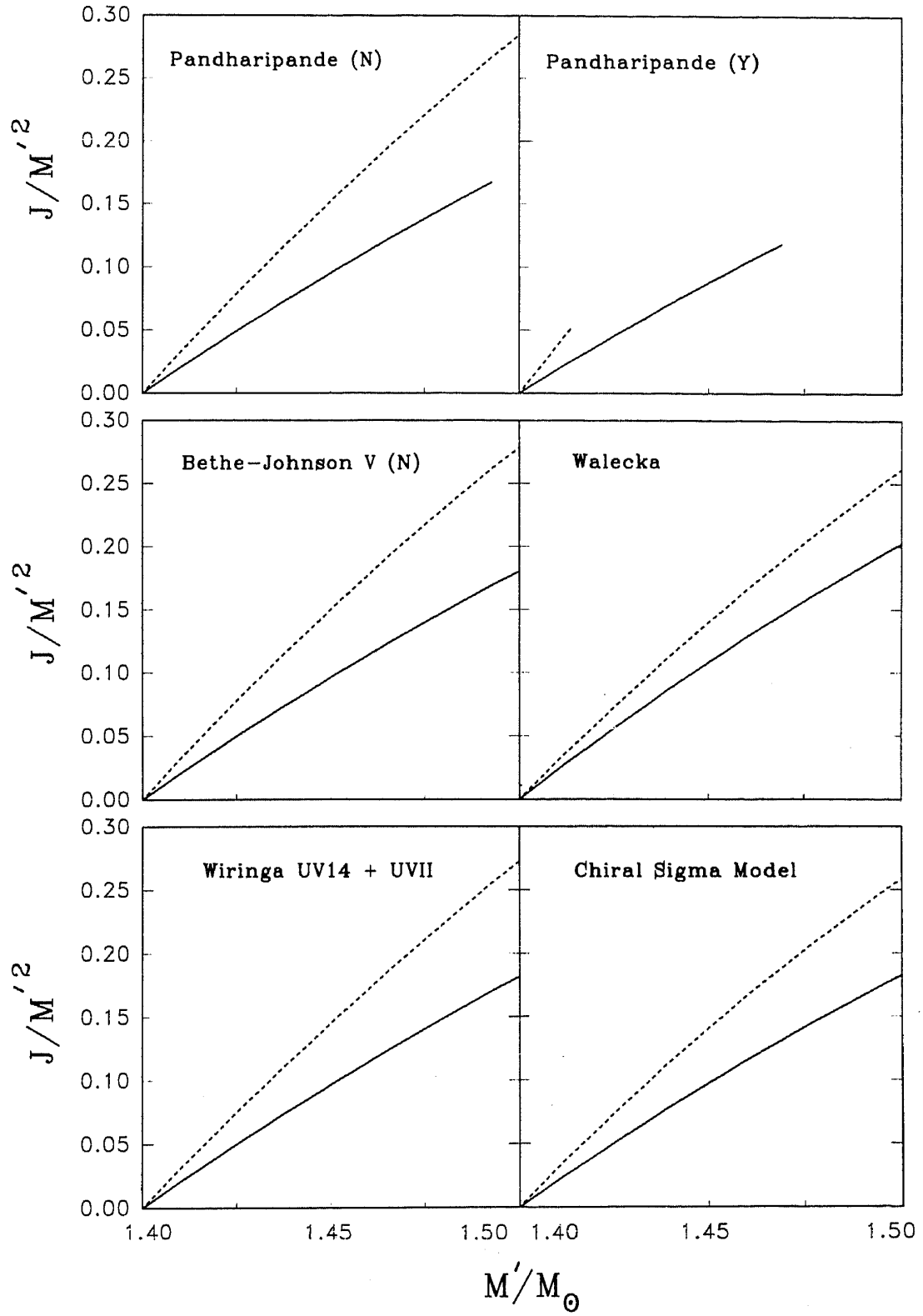

Figure 2. Evolution of the dimensionless angular momentum, $\tilde{j} = J/M^2$, of a neutron star with the accretion of mass, for six representative equations of state. The dashed curves correspond to the approach of KW, and the solid curves to our more self-consistent approach.

$M' = 1{\cdot}4\,M_\odot$ configuration. We integrate it either until $M' = M'_{\max}$, where $M'_{\max}$ is the mass corresponding to $J_{\max}$ or until $J = J_{\max}$ (the last entry for J in Table 3) whichever comes first.

The results of our computations for the angular momentum are illustrated in Fig. 2. The x-axis corresponds to $M'/M_\odot$ and the y-axis to J/M'^2. The dashed curves correspond to the angular momentum evolution computed in the fashion of KW, while the solid curves represent the results of the more self-consistent (numerical) estimates made by us as described above. The graphs indicate a slower rate of evolution of the accreting neutron star's angular momentum in the rotational case as compared to the case where rotational effects are not treated.

There are two factors contributing to the slower evolution of the angular momentum that we obtain. The less significant one is a comparatively smaller value of $\mathrm{d}M'_B/\mathrm{d}M'$. The more significant factor is that the angular momentum $\tilde{l}$ of the accreted particle is systematically less in the rotational case. Our calculations include the fact that infalling material co-rotating with the neutron star has a smaller cross-section for accretion than does counter-rotating infalling matter, so that the effective angular momentum is reduced (e.g., Misner, Thorne, & Wheeler 1974). Within the realm of overlap of our approximations, the results we find agree reasonably well with those of Cook *et al.* (1994a, b) for accretion induced changes of angular momentum.

5. Discussion

In presenting the results in the previous section, we have made the implicit assumption that the magnetic field of the neutron star is too small to affect accretion. Clearly, a quantitative estimate of this limit is in order. The Alfvén radius (r_A), is defined by the relationship (see Lamb, Pethick & Pines 1973)

$$\frac{B^2(r_A)}{8\pi} = \rho(r_A)v^2(r_A), \tag{39}$$

where ρ and v are respectively the density and radial velocity in the accretion disk, determines the location at which magnetic pressure channels the flow from a disk into an accretion column structure above the magnetic poles. Lamb, Pethick & Pines (1973) show that

$$r_A \lesssim 2{\cdot}6 \times 10^8 \left[\frac{\mu_{30}^{4/7}(M/M_\odot)^{1/7}}{L_{37}^{2/7}R_6^{2/7}}\right] \mathrm{cm}, \tag{40}$$

where $\mu_{30} = B_0R^3/10^{30}\,\mathrm{G\,cm^3}$, L_{37} is the total luminosity in units of $10^{37}\ \mathrm{erg\,s^{-1}}$, $R_6 = R/10^6\,\mathrm{cm}$ and B_0 is the magnetic field on the surface of the neutron star in gauss. The condition that $r_A < R$ implies that (taking $M = 1{\cdot}4\,M_\odot$ and $R_6 = 1$):

$$B_0 < 5{\cdot}5 \times 10^7 L_{37}^{1/2}, \tag{41}$$

and is necessary for the scenario we have discussed to be fully self-consistent, but fields somewhat higher than this value will not greatly modify our conclusions.

In our notation, $L = (E'_D + E'_S)\dot{M}c^2$, with $\dot{M}$ the accretion rate. According to our calculations, typical values for $(E'_D + E'_S)$ are of the order of 0·2. The luminosity $L_{37} = 1$

would then correspond to an accretion rate $\sim 5{\cdot}6 \times 10^{16}\,\mathrm{g\,s^{-1}}$. Such accretion rates are close to the ones estimated in X-ray binaries (Ghosh & Lamb 1991), so that our computations are relevant for systems with significant accretion on to old neutron stars whose surface magnetic fields have undergone substantial decay (to about $10^8\,G$).

Under these circumstances of weak neutron star magnetic fields, we have shown that an incorporation of rotational effects always increases the disk luminosity, usually decreases the boundary layer luminosity, and always reduces the rate at which the neutron star's angular momentum rises with accreted mass. These effects are large enough to merit their consideration in analyses of observations of low-mass X-ray binaries.

Acknowledgement

The authors thank Professor Ramesh Narayan for pointing out the role of spin-up energy correction in calculating the boundary layer luminosity. P. J. W. thanks the Director, Indian Institute of Astrophysics, for the hospitality extended to him. P. J. W.'s research in India is supported by the Smithsonian Institution through grant FR 10263600. This work was supported in part by NSF grant AST 91-02106 and by the Chancellor's Initiative Fund at Georgia State University. B. D. thanks the Director, Raman Research Institute for the kind hospitality.

References

Alpar M. A., Cheng, A. F., Ruderman, M. A., Shaham, J. 1982, *Nature*, **300** 728.
Arnett, W. D., Bowers, R. L. 1977, *Astrophys. J. Suppl.*, **33**, 415.
Baym, G., Pethick, C. J., Sutherland, P. G. 1971, *Astrophys. J.*, **170**, 299.
Bethe, H. A., Johnson, M. B. 1974, *Nucl. Phys.* **A230**, 1.
Bhattacharya, D., van den Heuvel, E. P. J. 1991, *Phys. Rep.*, **203** 1.
Chandrasekhar, S. 1969, *Ellipsoidal Figures of Equilibrium* (New Haven: Yale University Press).
Cook, G. B., Shapiro, S. L., Teukolsky, S. A. 1994a, *Astrophys. J.*, **423**, L117.
Cook, G. B., Shapiro, S. L., Teukolsky, S. A. 1994b, *Astrophys. J.*, **424**, 823.
Datta, B., Ray, A. 1983, *Mon. Not. R. astr. Soc.*, **204**, 75.
Datta, B. 1988, *Fund. Cosmic Phys.*, **12**, 151.
Datta, B., Thampan, A. V., Bhattacharya, D. 1995, *J. Astrophys. Astr.*, **16**, 375.
Feynman, R. P., Metropolis, N., Teller, E., 1949, *Phys. Rev.*, **75**, 1561.
Ghosh, P., Lamb, F. K., Pethick, C. J. 1977, *Astrophys. J.*, **217**, 578.
Ghosh, P., Lamb, F. K. 1991 in *Neutron Stars: Theory and Observations*, eds. J. Ventura & D. Pines, (Dordrecht: Kluwer Acad. Publ.) p. 363.
Hartle, J. B., Thorne, K. S. 1968, *Astrophys. J.*, **153**, 807 (HT).
Kley, W. 1991, *Astr. Astrophys.*, **247**, 95.
Kluźniak, W., Wagoner, R. V. 1985, *Astrophys. J.*, **297**, 548 (KW).
Kluźniak, W. 1987, *Ph. D. Thesis*, Stanford Univ.
Lamb, F. K., Pethick, C. J., Pines, D. 1973, *Astrophys. J.*, **184**, 271.
Misner, C. W., Thorne, K. S., Wheeler, J. A. 1974, *Gravitation* (San Francisco: Freeman).
Negele, J. W., Vautherin, D. 1973, *Nucl. Phys.*, **A207**, 298.
Paczyński, B. 1987, *Nature*, **327** 303.
Pandharipande, V. R. 1971a, *Nucl. Phys.*, **A174**, 641.
Pandharipande, V. R. 1971b, *Nucl. Phys.*, **A178**, 123.
Papaloizou, J. C. B., Stanley, G. Q. G. 1986, *Mon. Not. R. astr. Soc.*, **220**, 593.
Popham, R., Narayan, R. 1995, *Astrophys. J.*, **442**, 337.

Priedhorsky, W. 1986, *Astrophys. J.*, **306**, L97.
Radhakrishnan, V., Srinivasan, G. 1982, *Current Sci.*, **51**, 1096.
Sahu, P. K., Basu, R., Datta, B. 1993, *Astrophys. J.*, **416**, 267.
Syunyaev, R. A., Shakura, N. I. 1986, *Sov. Astr. Lett.*, **12**, 117 (SS).
van Paradijs, J. 1991 in *Neutron Stars: Theory and Observations*, Eds. J. Ventura & D. Pines, (Dordrecht: Kluwer Acad. Publ.), p. 245.
Walecka, J. D. 1974, *Ann. Phys.*, **83**, 491.
Wiringa, R. B., Fiks, V., Fabrocini, A. 1988, *Phys. Rev. C*, **38**, 1010.